

Electronic Supplementary Information

Infrared spectroscopy and theoretical structure analyses of protonated fluoroalcohol clusters: An impact of the fluorination on the hydrogen bond networks

Takahiro Shinkai,^{1‡} Po-Jen Hsu,^{2‡} Asuka Fujii,^{*1} and Jer-Lai Kuo^{*2}

¹Department of Chemistry, Graduate School of Science, Tohoku University,

Sendai 980-8578, Japan

²Institute of Atomic and Molecular Sciences, Academia Sinica, Taipei 10617, Taiwan

E-mail: asuka.fujii.c5@tohoku.ac.jp (A.F.), jlkuo@pub.iams.sinica.edu.tw (J.-L.K.).

‡ Takahiro Shinkai and Po-Jen Hsu contributed equally to this study.

Contents

- Table S1.** The number of distinct stable isomers searched for the bare, Ar-tagged, Ar₂-tagged, and Ne-tagged clusters of H⁺(TFE)_n for n = 4 and 5 using M06-2X/6-311+G(d,p).
- Table S2.** The number of distinct stable isomers searched for the bare, Ar-tagged, and Ne-tagged clusters of H⁺(TFE)_n for n = 4 and 5 using B3LYP+D3/6-31+G(d).
- Table S3.** Proton affinities of molecules related in the present study

- Figure S1.** Comparison of the observed IR spectra of bare $\text{H}^+(\text{EtOH})_n$ and bare $\text{H}^+(\text{TFE})_n$ in the size range of $n = 4 - 7$.
- Figure S2.** Comparison of the observed IR spectra of $\text{H}^+(\text{EtOH})_n\text{-Ar}$ and $\text{H}^+(\text{TFE})_n\text{-Ar}$ in the size range of $n = 4 - 7$.
- Figure S3.** Observed spectra of $\text{H}^+(\text{TFE})_n\text{-Ar}$, $\text{H}^+(\text{TFE})_n\text{-Ar}_2$, and $\text{H}^+(\text{TFE})_n\text{-Ne}$ of $n = 4$ and 5 .
- Figure S4.** Relative zero-point corrected energies of $\text{H}^+(\text{TFE})_4$ and $\text{H}^+(\text{TFE})_{4\text{-X}}$ ($\text{X}=\text{Ne}$, Ar , and Ar_2) using $\text{M06-2X/6-311+G(d,p)}$.
- Figure S5.** Relative zero-point corrected energies of $\text{H}^+(\text{TFE})_5$ and $\text{H}^+(\text{TFE})_{5\text{-X}}$ ($\text{X}=\text{Ne}$, Ar , and Ar_2) using $\text{M06-2X/6-311+G(d,p)}$.
- Figure S6.** Comparison between the observed IR spectra of $\text{H}^+(\text{TFE})_n\text{-Ar}$ clusters and the Q-HSA simulated IR spectra of *bare* $\text{H}^+(\text{TFE})_n$ at $\text{M06-2X/6-311+G(d,p)}$ for $n = 4$ and 5 .
- Figure S7.** Relative zero-point corrected energies of $\text{H}^+(\text{TFE})_4$ and $\text{H}^+(\text{TFE})_{4\text{-X}}$ ($\text{X}=\text{Ne}$ or Ar) using $\text{B3LYP+D3/6-31+G(d)}$.
- Figure S8.** Relative zero-point corrected energies of $\text{H}^+(\text{TFE})_5$ and $\text{H}^+(\text{TFE})_{5\text{-X}}$ ($\text{X}=\text{Ne}$ or Ar) using $\text{B3LYP+D3/6-31+G(d)}$.
- Figure S9.** Comparison between the observed IR spectra and the Q-HSA simulated IR spectra of $\text{B3LYP+D3/6-31+G(d)}$ for *bare* and *tagged* $\text{H}^+(\text{TFE})_4$ clusters.
- Figure S10.** Comparison between the observed IR spectra and the Q-HSA simulated IR spectra of $\text{B3LYP+D3/6-31+G(d)}$ for *bare* and *tagged* $\text{H}^+(\text{TFE})_5$ clusters.
- Figure S11.** The minimum free energy structures of *bare* $\text{H}^+(\text{TFE})_6$ and $\text{H}^+(\text{TFE})_7$ clusters using $\text{B3LYP+D3/6-31+G(d)}$.
- Figure S12.** The schematic diagram for the intermolecular $\text{F}\dots\text{H-O}$ angle and the intramolecular H-O-C-C dihedral angle.
- Figure S13.** The $\text{F}\dots\text{H-O}$ angles for the free OH sites versus free OH stretching frequencies in the stable L structures of $\text{H}^+(\text{TFE})_4$ and $\text{H}^+(\text{TFE})_{4\text{-X}}$ ($\text{X}=\text{Ne}$, Ar , or Ar_2) using $\text{M06-2X/6-311+G(d,p)}$ (with color coded $\text{F}\dots\text{H}$ distances).
- Figure S14.** The $\text{F}\dots\text{H-O}$ bond angles for the free OH sites versus free OH stretching frequencies in the stable L structures of $\text{H}^+(\text{TFE})_4$ and $\text{H}^+(\text{TFE})_{4\text{-X}}$ ($\text{X}=\text{Ne}$, Ar , or Ar_2) using $\text{M06-2X/6-311+G(d,p)}$ (with color coded $\text{X}\dots\text{H-O}$ angles).
- Figure S15.** The H-O-C-C dihedral angles for the free OH sites versus free OH stretching frequencies in the stable L structures of $\text{H}^+(\text{TFE})_4$ and $\text{H}^+(\text{TFE})_{4\text{-X}}$ ($\text{X}=\text{Ne}$, Ar , or Ar_2) using $\text{M06-2X/6-311+G(d,p)}$ (with color

coded F...H distances).

- Figure S16.** The H-O-C-C dihedral angles for the free OH sites versus free OH stretching frequencies in the stable L structures of $\text{H}^+(\text{TFE})_4$ and $\text{H}^+(\text{TFE})_4\text{-X}$ (X=Ne, Ar, or Ar_2) using M06-2X/6-311+G(d,p) (with color coded X...H-O angles).
- Figure S17.** The F...H-O angles for the free OH sites versus free OH stretching frequencies in the stable L structures of $\text{H}^+(\text{TFE})_5$ and $\text{H}^+(\text{TFE})_5\text{-X}$ (X=Ne, Ar, or Ar_2) using M06-2X/6-311+G(d,p) (with color coded F...H distances).
- Figure S18.** The F...H-O angles for the free OH sites versus free OH stretching frequencies in the stable L structures of $\text{H}^+(\text{TFE})_5$ and $\text{H}^+(\text{TFE})_5\text{-X}$ (X=Ne, Ar, or Ar_2) using M06-2X/6-311+G(d,p) (with color coded X...H-O angles).
- Figure S19.** The H-O-C-C dihedral angles for the free OH sites versus free OH stretching frequencies in the stable L structures of $\text{H}^+(\text{TFE})_5$ and $\text{H}^+(\text{TFE})_5\text{-X}$ (X=Ne, Ar, or Ar_2) using M06-2X/6-311+G(d,p) (with color coded F...H distances).
- Figure S20.** The H-O-C-C dihedral angles for the free OH sites versus free OH stretching frequencies in the stable L structures of $\text{H}^+(\text{TFE})_5$ and $\text{H}^+(\text{TFE})_5\text{-X}$ (X=Ne, Ar, or Ar_2) using M06-2X/6-311+G(d,p) (with color coded X...H-O angles).
- Figure S21.** The structures of *bare* and *tagged* $\text{H}^+(\text{TFE})_4$ clusters with minimum free energy using B3LYP+D3/6-31+G(d).
- Figure S22.** The structures of *bare* and *tagged* $\text{H}^+(\text{TFE})_5$ clusters with minimum free energy using B3LYP+D3/6-31+G(d).
- Figure S23.** Infrared spectra of $\text{H}^+(\text{DFE})_n$ and $\text{H}^+(\text{DFE})_n\text{-Ar}$ in the size range of $n = 4 - 7$.

Table S1. The number of distinct stable isomers searched for the bare, Ar-tagged, Ar₂-tagged, and Ne-tagged clusters of H⁺(TFE)_{*n*} for *n* = 4 and 5 using M06-2X/6-311+G(d,p).

H ⁺ (TFE) _{<i>n</i>}	Bare	Ar-tagged	Ar ₂ -tagged	Ne-tagged
<i>n</i> = 4	578	561	705	573
<i>n</i> = 5	578	1088	1169	808

Table S2. The number of distinct stable isomers searched for the bare, Ar-tagged, and Ne-tagged clusters of $\text{H}^+(\text{TFE})_n$, for $n = 4$ and 5 using B3LYP+D3/6-31+G(d). The rare gas atom tagged spectra simulated by B3LYP+D3 did not show a good agreement with the observed spectra in the free OH region (see the free OH stretch bands in Figs. S9 and S10). Therefore, the Ar_2 -tagged clusters were not searched.

$\text{H}^+(\text{TFE})_n$	Bare	Ar-tagged	Ne-tagged
$n = 4$	383	419	422
$n = 5$	751	682	689

Table S3. Proton affinities of molecules related in the present study (in kJ/mol)

	TFE ^{a)}	DFE ^{b)}	DFP ^{c)}	TFP ^{d)}	methanol	ethanol
Exp. ^{e)}	700.2	727.4	–	–	754.4	776
Calc. ^{f)}	722	746	762	802	800	–

a)2,2,2-trifluoroethanol, b)2,2-difluoroethanol, c)2,2-difluoropropanol,
d)3,3,3-trifluoropropanol, e) Ref. 25 in the main text, f) PBE1PB/6-311+G.

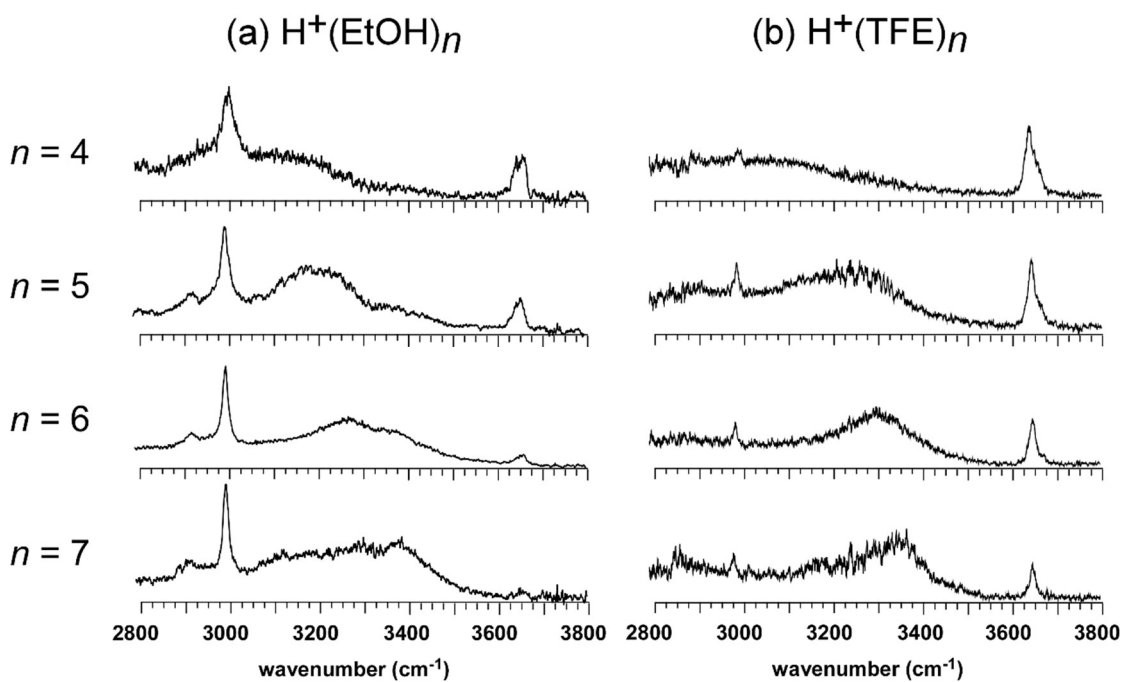


Figure S1. Comparison of the observed IR spectra of (a) bare $\text{H}^+(\text{ethanol})_n$ ($\text{H}^+(\text{EtOH})_n$) and (b) bare $\text{H}^+(\text{TFE})_n$ in the size range of $n = 4 - 7$. The spectra of $\text{H}^+(\text{EtOH})_n$ are taken from Ref. 13. The spectra of $\text{H}^+(\text{TFE})_n$ are reproduction of those shown in Figure 2(a) in the main text. The main spectral features are attributed to free ($> 3600 \text{ cm}^{-1}$) and H-bonded ($< 3600 \text{ cm}^{-1}$) OH stretches. Sharp bands in the $2900 - 3000 \text{ cm}^{-1}$ region are CH stretches. The spectral features of $\text{H}^+(\text{EtOH})_n$ are very similar to those of $\text{H}^+(\text{TFE})_n$ of the corresponding size, indicating that the H-bond network structures are common between these two cluster species. The L-type structures of the observed bare (warm) $\text{H}^+(\text{EtOH})_n$ have been established (see the main text of Ref. 13).

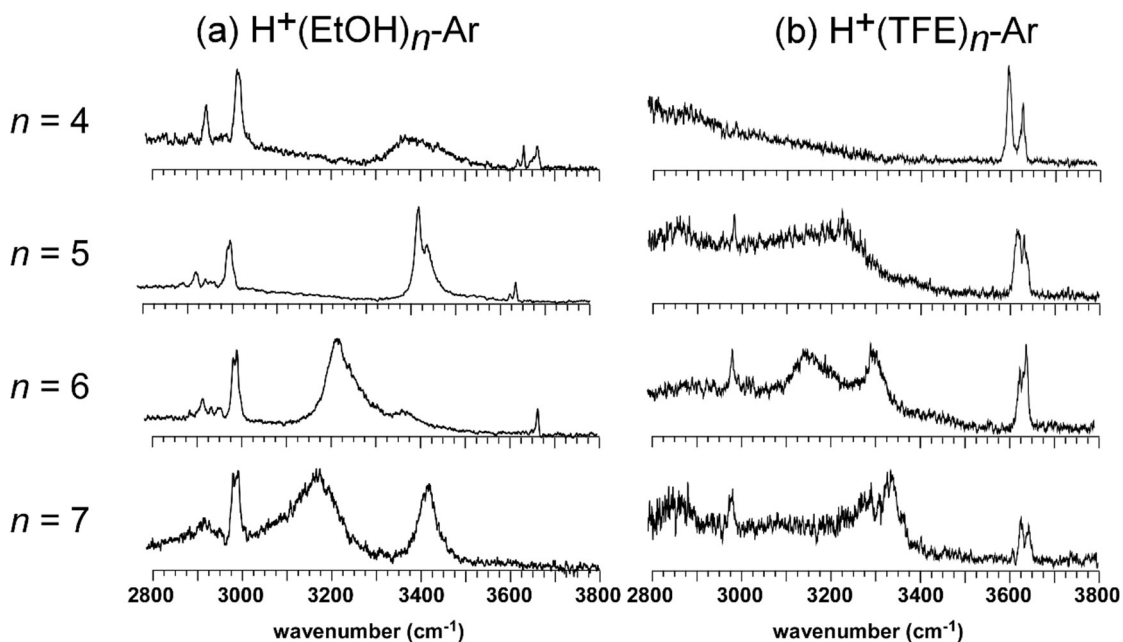


Figure S2. Comparison of the observed IR spectra of (a) $\text{H}^+(\text{EtOH})_n\text{-Ar}$ and (b) $\text{H}^+(\text{TFE})_n\text{-Ar}$ in the size range of $n = 4 - 7$. The spectra of $\text{H}^+(\text{EtOH})_n\text{-Ar}$ are taken from Ref. 13. The spectra of $\text{H}^+(\text{TFE})_n\text{-Ar}$ are reproduction of those shown in Figure 2(b) of the main text. In contrast with the case of the bare (warm) clusters, the spectral features of the Ar tagged (cold) $\text{H}^+(\text{EtOH})_n$ are very different from those of $\text{H}^+(\text{TFE})_n\text{-Ar}$ in all the sizes. This indicates that the H-bond network structures are totally different between the most stable isomers of these two cluster species. It has been established that the observed spectra of $\text{H}^+(\text{EtOH})_n\text{-Ar}$ ($n = 4 - 7$) are attributed to the **L/C** (coexistence), **C**, **Ct**, and **bC** type structures, respectively (see the main text of Ref. 13).

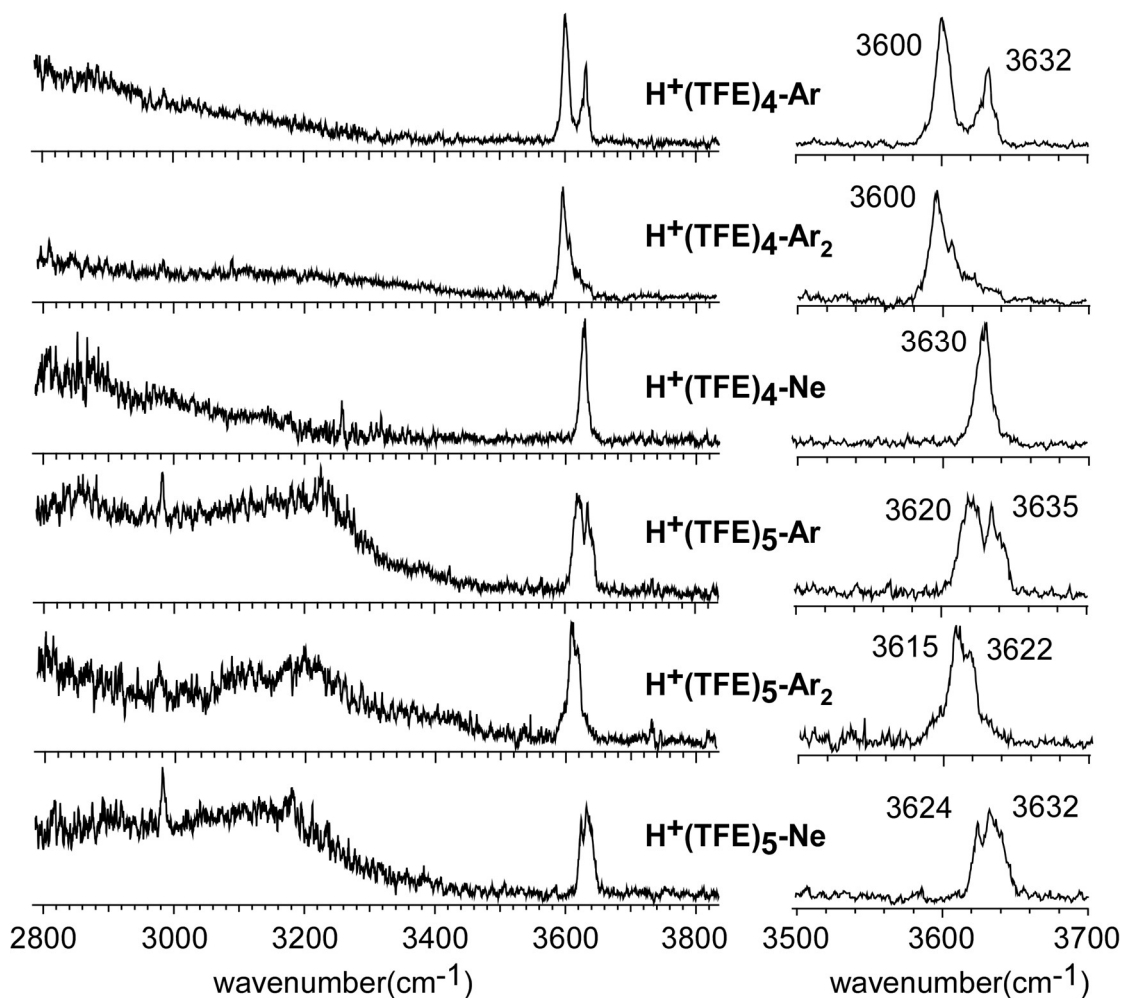


Figure S3. Observed spectra of $\text{H}^+(\text{TFE})_n\text{-Ar}$, $\text{H}^+(\text{TFE})_n\text{-Ar}_2$, and $\text{H}^+(\text{TFE})_n\text{-Ne}$ of $n = 4$ and 5. The spectra of the right column are the expansion of the free OH stretch region. The gross feature of the spectra does not depend on the tag species. This means that the H-bond network type is common in these three tagged clusters. On the other hand, the free OH band position and its splitting depend on the tag.

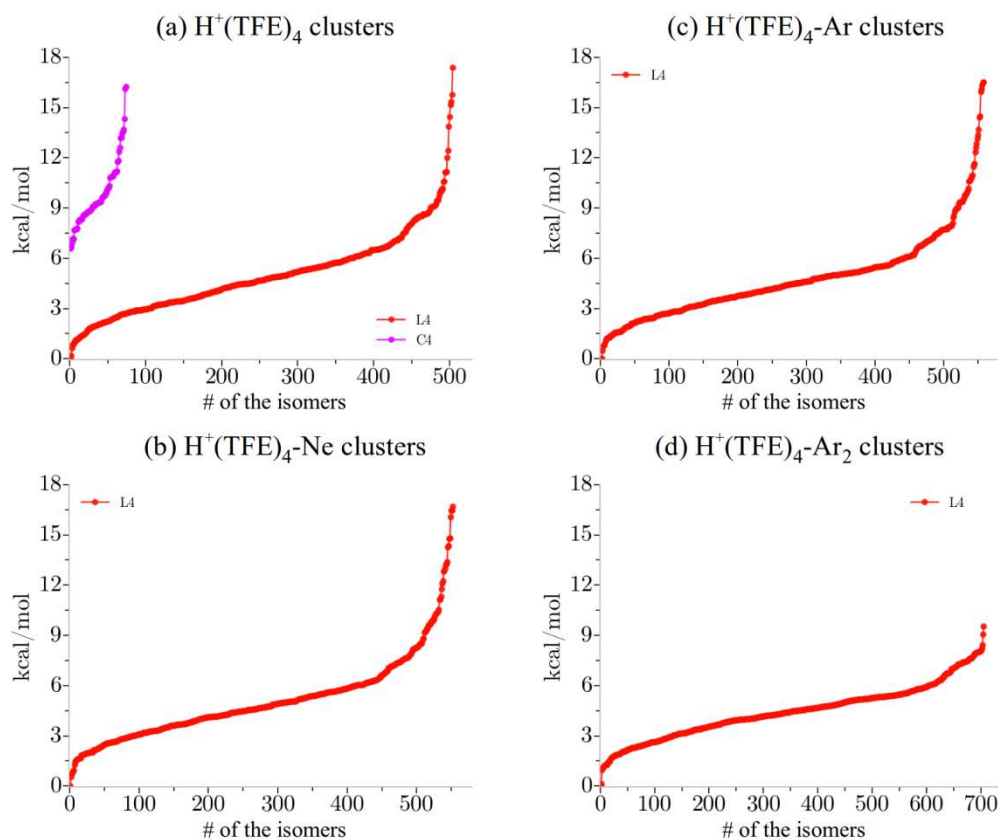


Figure S4. Relative zero-point corrected energies of (a) H⁺(TFE)₄, (b) H⁺(TFE)₄-Ne, (c) H⁺(TFE)₄-Ar, and (d) H⁺(TFE)₄-Ar₂ using M06-2X/6-311+G(d,p) for geometric optimization and frequency calculation. The abscissa is the numbering of the isomers. The H-bonded structures are labeled by **L4** (linear, red) and **C4** (cyclic, magenta).

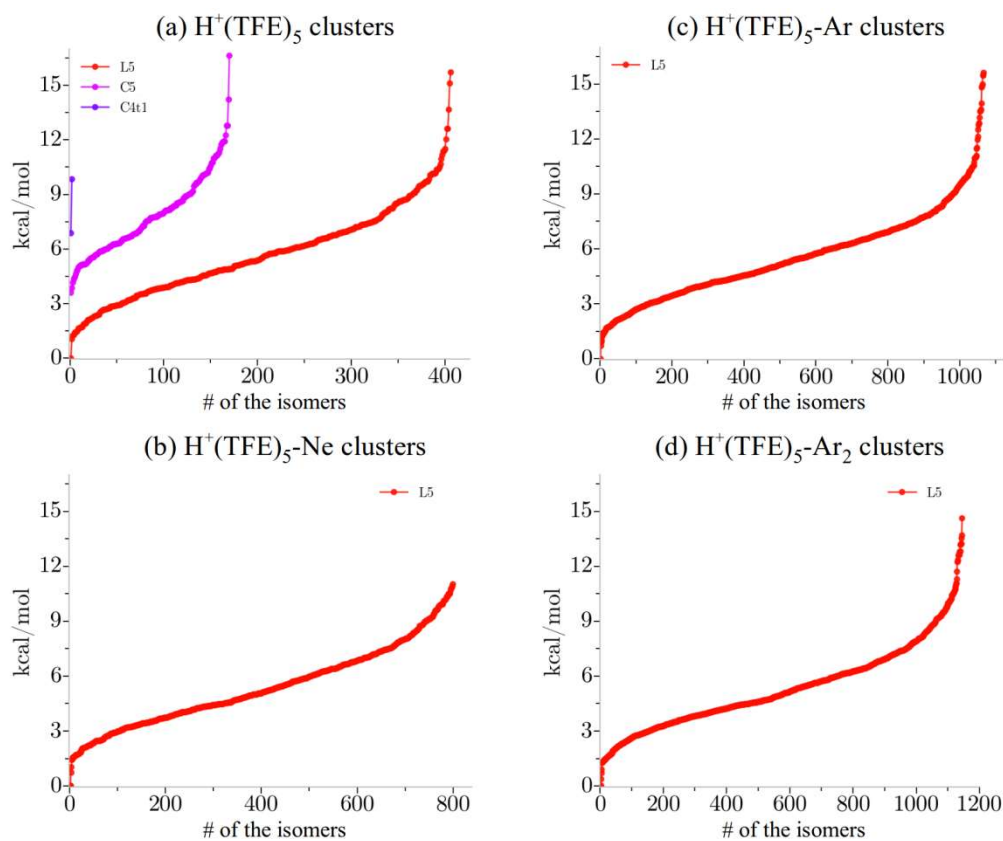


Figure S5. Relative zero-point corrected energies of (a) $H^+(TFE)_5$, (b) $H^+(TFE)_5$ -Ne, (c) $H^+(TFE)_5$ -Ar, and (d) $H^+(TFE)_5$ -Ar₂ clusters using M06-2X/6-311+G(d,p) for geometric optimization and frequency calculation. The abscissa is the numbering of the isomers. The H-bonded structures are labeled by **L5** (linear, red) and **C5** (cyclic, magenta).

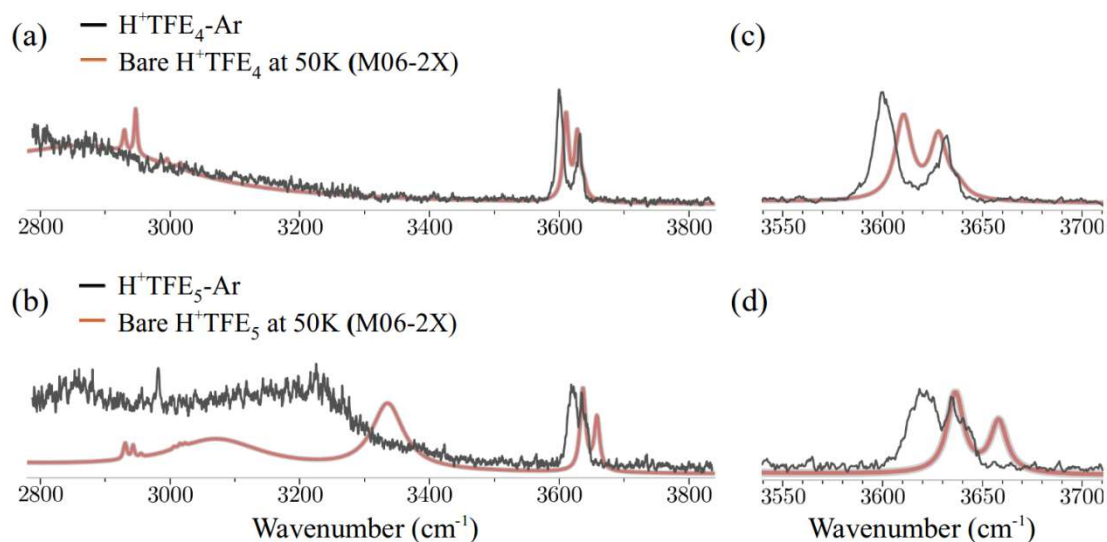


Figure S6. Comparison between the observed IR spectra (black traces) of $\text{H}^+(\text{TFE})_n\text{-Ar}$ clusters and the Q-HSA simulated IR spectra (red trace) of *bare* $\text{H}^+(\text{TFE})_n$ at 50 K for (a) $n = 4$ and (b) $n = 5$. The zoom-in spectra in the free OH stretch region for $n = 4$ and 5 are shown in (c) and (d), respectively. Only linear H-bonded structures are essentially involved in the Q-HSA at 50K.

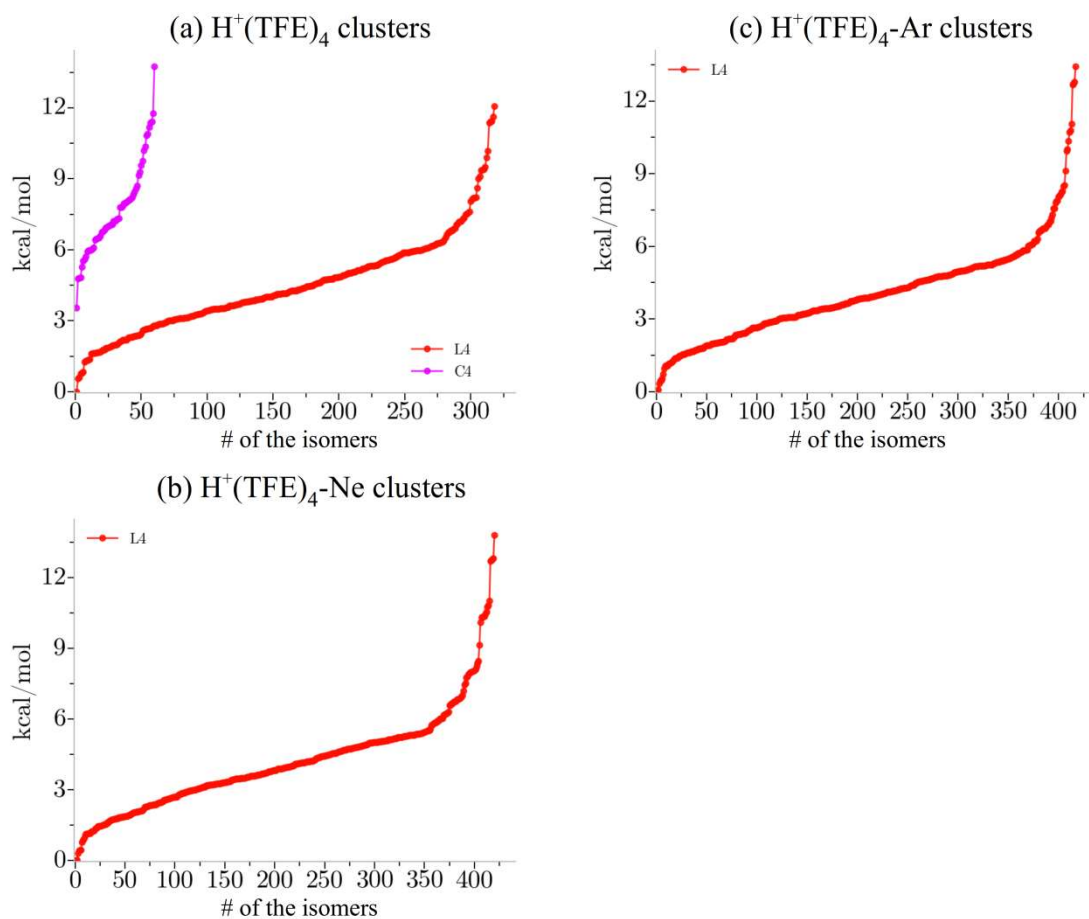


Figure S7. Relative zero-point corrected energies of (a) $\text{H}^+(\text{TFE})_4$, (b) $\text{H}^+(\text{TFE})_4\text{-Ne}$, and (c) $\text{H}^+(\text{TFE})_4\text{-Ar}$ using B3LYP+D3/6-31+G(d) for geometric optimization and frequency calculation. The abscissa is the numbering of the isomers. The H-bonded structures are labeled by L4 (linear, red) and C4 (cyclic, magenta).

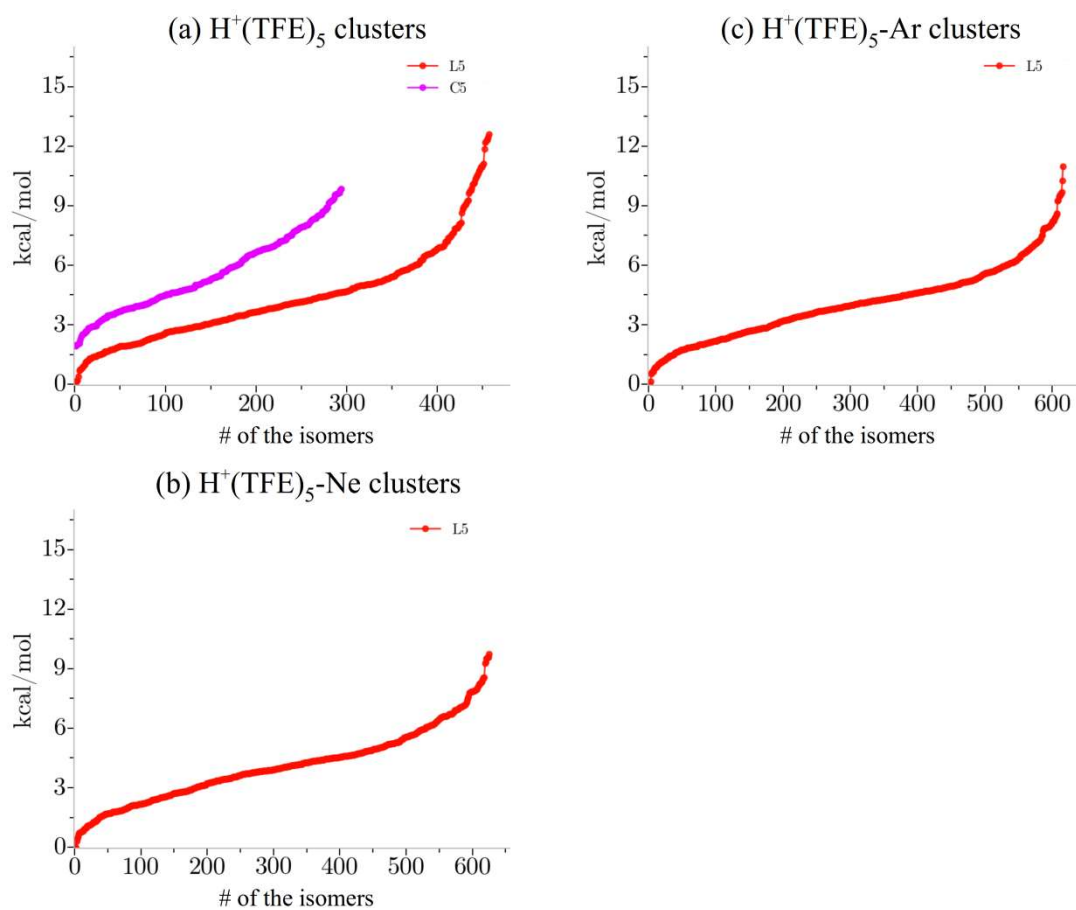


Figure S8. Relative zero-point corrected energies of (a) $H^+(TFE)_5$, (b) $H^+(TFE)_5$ -Ne, and (c) $H^+(TFE)_5$ -Ar using B3LYP+D3/6-31+G(d) for geometric optimization and frequency calculation. The abscissa is the numbering of the isomers. The H-bonded structures are labeled by L4 (linear, red) and C4 (cyclic, magenta).

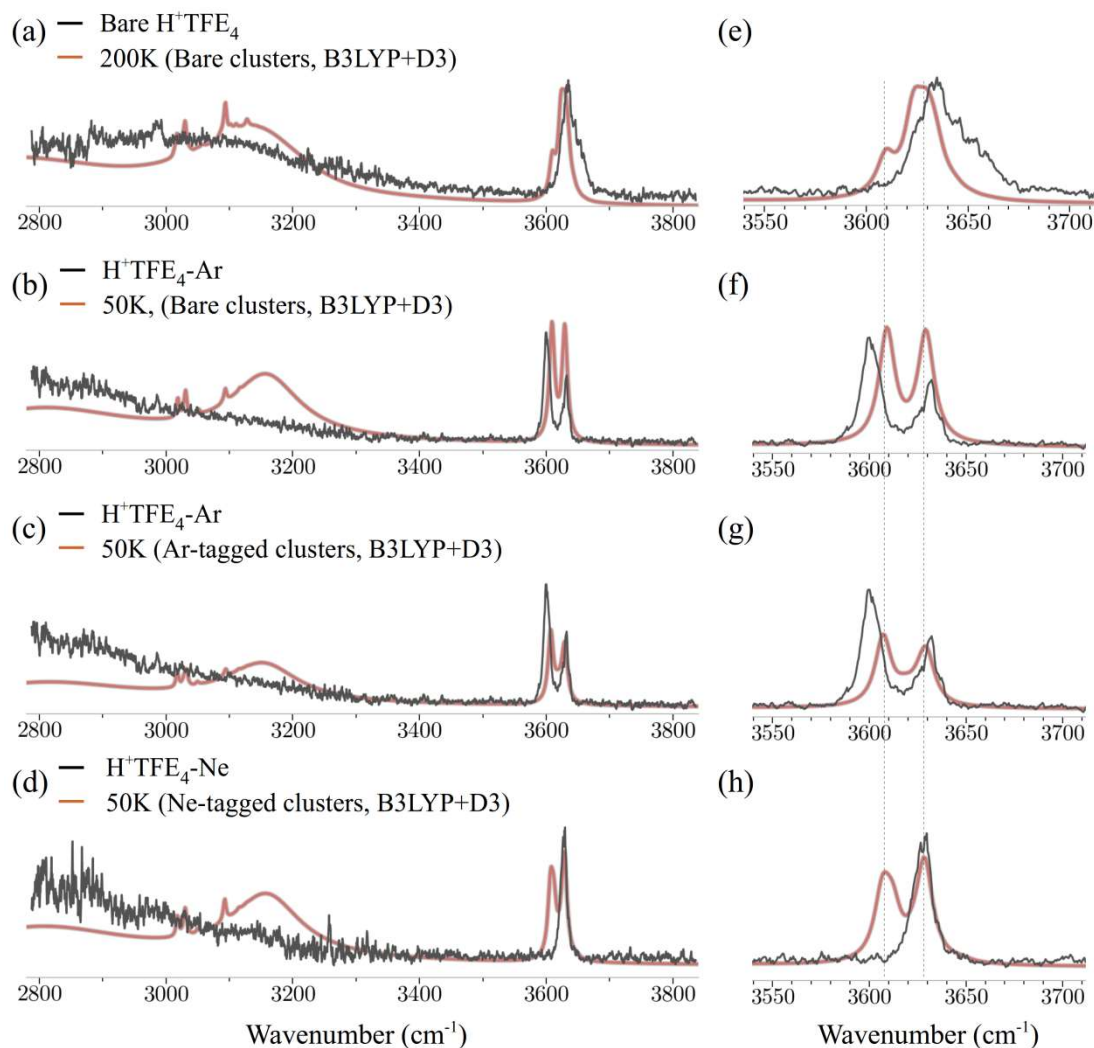


Figure S9. Comparison between the observed IR spectra (black traces) and the Q-HSA simulated IR spectra (red traces) of B3LYP+D3/6-31+G(d) (B3LYP+D3) for $\text{H}^+(\text{TFE})_4$ and $\text{H}^+(\text{TFE})_4\text{-X}$ ($\text{X} = \text{Ar}$ or Ne). In the Q-HSA simulations, frequencies were scaled by 0.973. Clusters without a tagged atom were used for the comparison of (a) bare $\text{H}^+(\text{TFE})_4$ and (b) $\text{H}^+(\text{TFE})_4\text{-Ar}$. The Ar-tagged and Ne-tagged clusters of B3LYP+D3 minima were used for (c) $\text{H}^+(\text{TFE})_4\text{-Ar}$, and (d) $\text{H}^+(\text{TFE})_4\text{-Ne}$, respectively. The zoom-in spectra in the free OH stretch region are shown in (e) – (h). The best match temperatures in the simulated spectra are 200K for the bare clusters and 50K for all the tagged clusters. Only linear H-bonded structures are essentially involved in the Q-HSA for these temperatures.

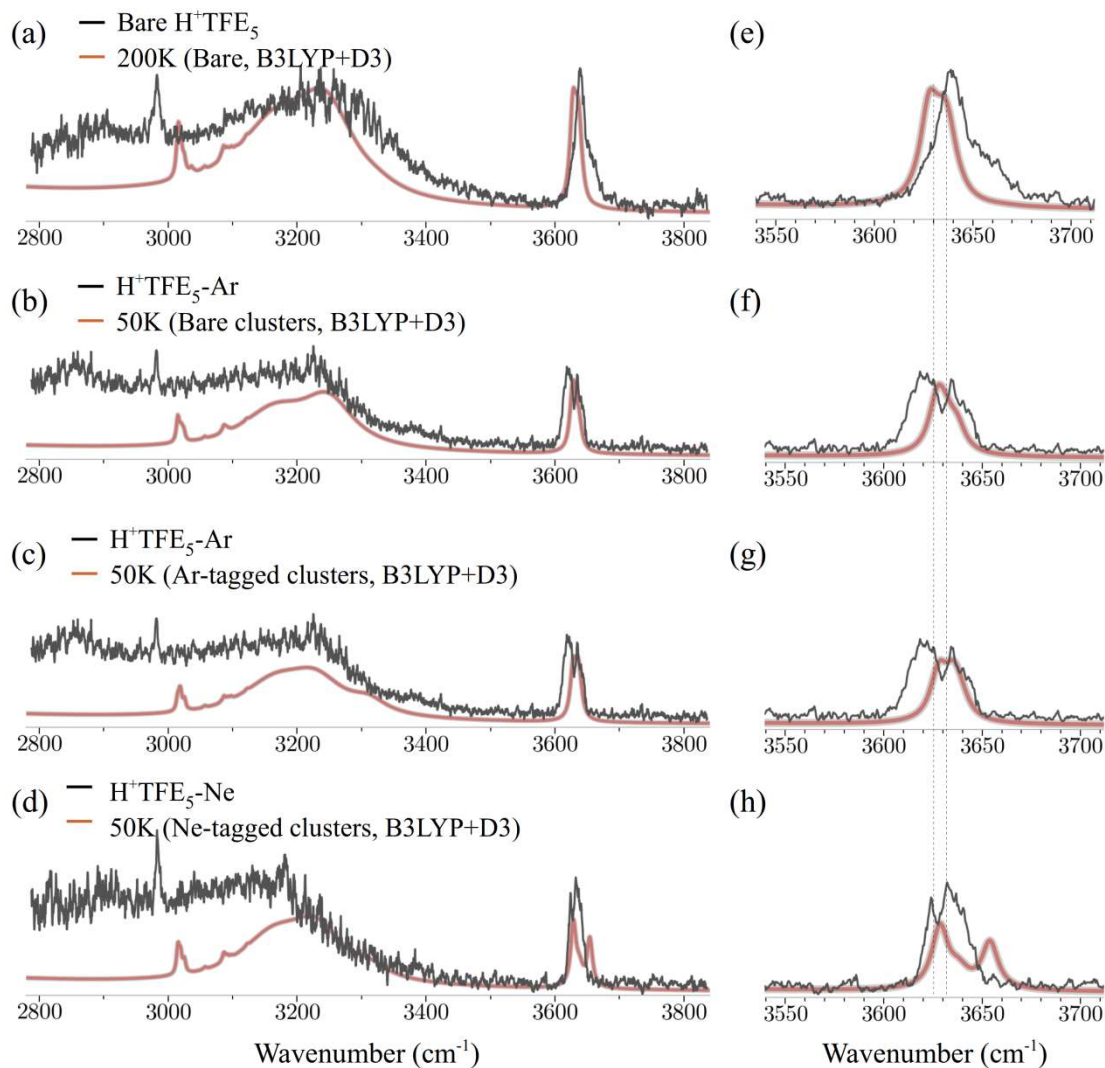


Figure S10. Comparison between the observed IR spectra (black traces) and the Q-HSA simulated IR spectra (red traces) of B3LYP+D3/6-31+G(d) (B3LYP+D3) for $\text{H}^+(\text{TFE})_5$ and $\text{H}^+(\text{TFE})_5\text{-X}$ ($\text{X} = \text{Ar}$ or Ne). In the Q-HSA simulations, frequencies were scaled by 0.973. Optimized clusters without a tagged atom were used for the comparison of (a) bare $\text{H}^+(\text{TFE})_5$ and (b) $\text{H}^+(\text{TFE})_5\text{-Ar}$. The Ar-tagged and Ne-tagged clusters of B3LYP+D3 minima were used for (c) $\text{H}^+(\text{TFE})_5\text{-Ar}$, and (d) $\text{H}^+(\text{TFE})_5\text{-Ne}$, respectively. The zoom-in spectra in the free OH stretch region are shown in (e) – (h). The best match temperatures in the simulated spectra are 200K for the bare clusters and 50K for all the tagged clusters. Only linear H-bonded structures are essentially involved in the Q-HSA for these temperatures.

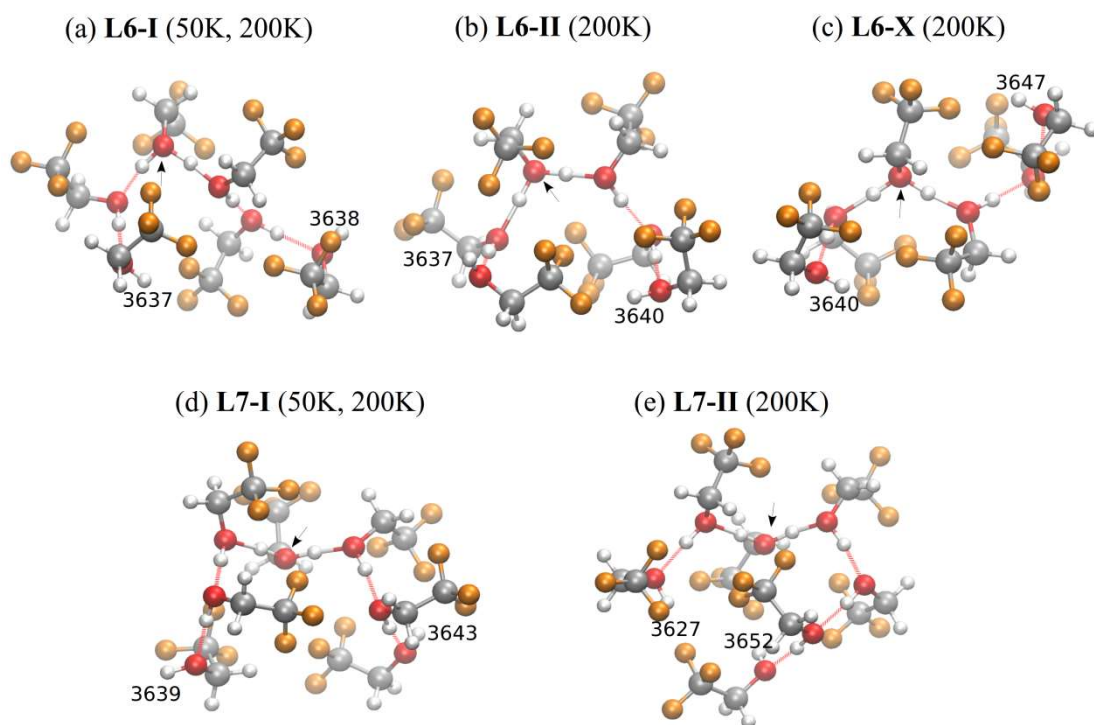


Figure S11. The structures of (a) - (c) bare $\text{H}^+(\text{TFE})_6$ and (d)/(e) $\text{H}^+(\text{TFE})_7$ clusters with minimum free energy at 50K and 200K using B3LYP+D3 level of theory. The arrow indicates the location of the protonated site. The numbers near the free OH sites indicate the scaled harmonic frequencies of free OH stretching modes in cm^{-1} .

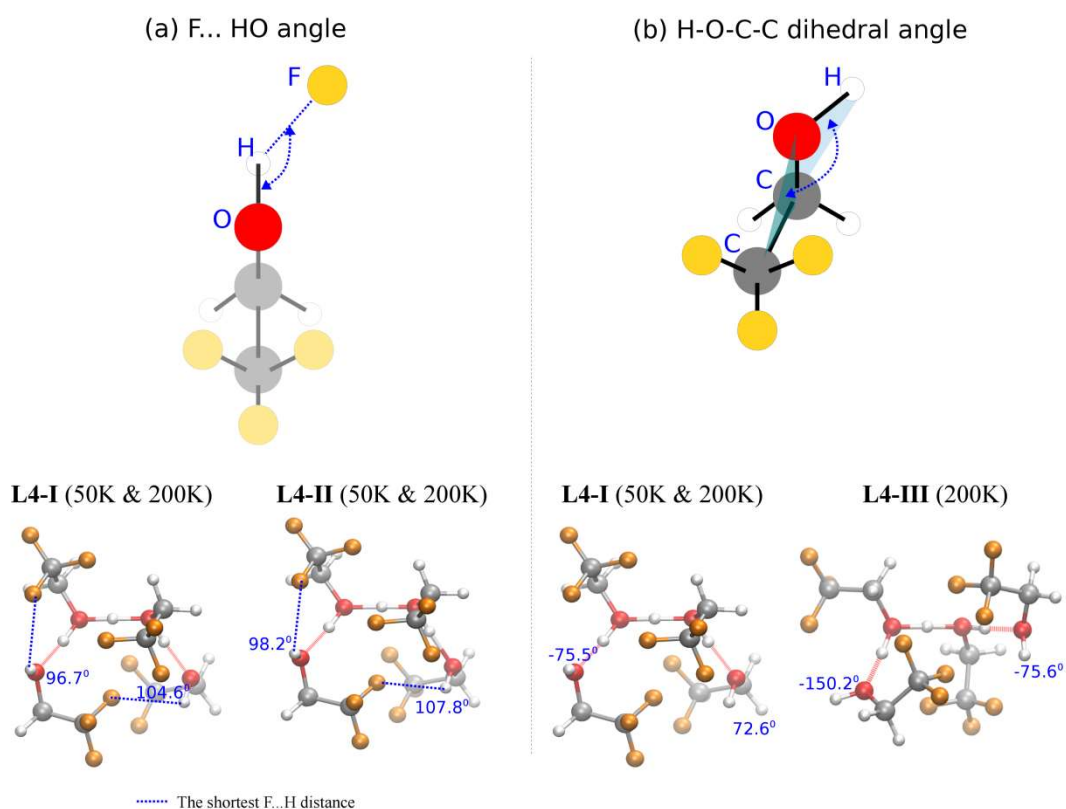


Figure S12. The schematic diagram for (a) the intermolecular F...H-O angle and (b) the intramolecular H-O-C-C dihedral angle. The nearest F atom to the free OH site was chosen for the former as shown in the **L4-I** and **L4-II** structures. The trans rotamer (150 – 180 or -150 – -180 degrees) can be seen in **L4-III**. The others are g+ (60 – 90 degrees) and g- (-60 – -90 degrees) rotamers. The definitions of the two angles were applied to Figures 8 and S13-S20.

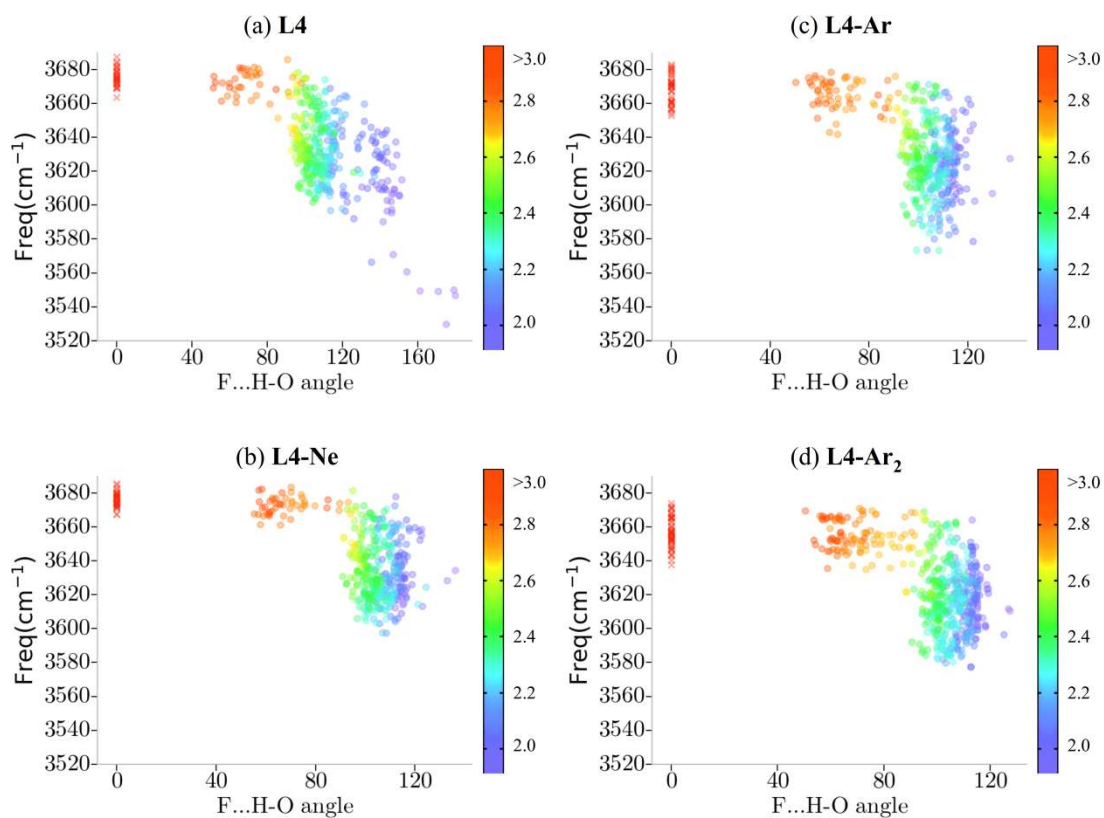


Figure S13. The F...H-O angles (abscissa) for the free OH sites versus free OH stretching frequencies (ordinate) in the stable L structures of (a) $\text{H}^+(\text{TFE})_4$, (b) $\text{H}^+(\text{TFE})_4\text{-Ne}$, (c) $\text{H}^+(\text{TFE})_4\text{-Ar}$, and (d) $\text{H}^+(\text{TFE})_4\text{-Ar}_2$ using M06-2X/6-311+G(d,p). The energies of the data points are within 5 kcal/mol to the most stable structure. The color code represents the distance between the F atom and the H atom of the free OH site from smaller than 2 Å (purple) to larger than 3 Å (red). The red cross symbol represents the absence of the F atom to the free OH site using 3.5 Å as the cut-off distance.

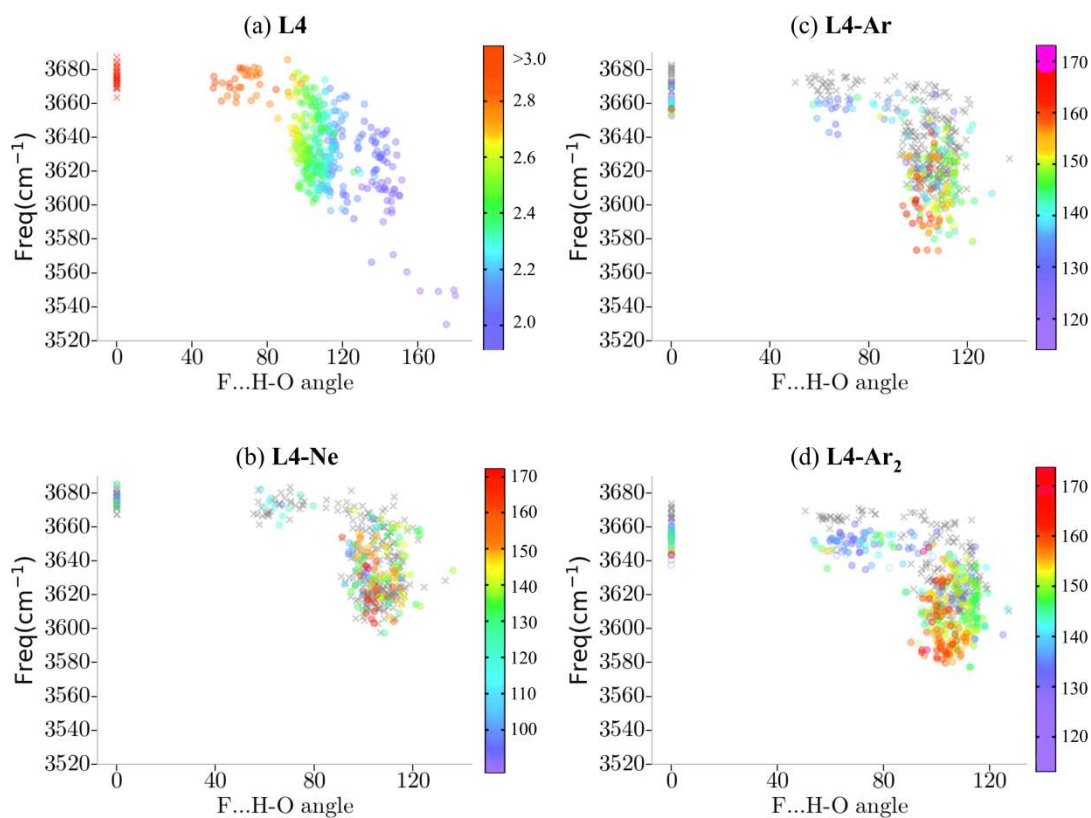


Figure S14. The F...H-O angles (abscissa) for the free OH sites versus free OH stretching frequencies (ordinate) in the stable L structures of (a) $\text{H}^+(\text{TFE})_4$ (same as Fig. S13(a)), (b) $\text{H}^+(\text{TFE})_4\text{-Ne}$, (c) $\text{H}^+(\text{TFE})_4\text{-Ar}$ and (d) $\text{H}^+(\text{TFE})_4\text{-Ar}_2$ using M06-2X/6-311+G(d,p). The data points are the same as Figure S13, but the definition of the color code in (b) – (d) is changed. The color code in (b) - (d) represents the X...H-O angles (X=Ne, Ar, or Ar_2) from smaller than 90 degrees for X=Ne and 130 degrees for X=Ar and Ar_2 (purple) to larger than 160 degrees (red). The gray cross symbol shows the absence of the tagged atom to the free OH site using 2.8 Å as the cut-off distance.

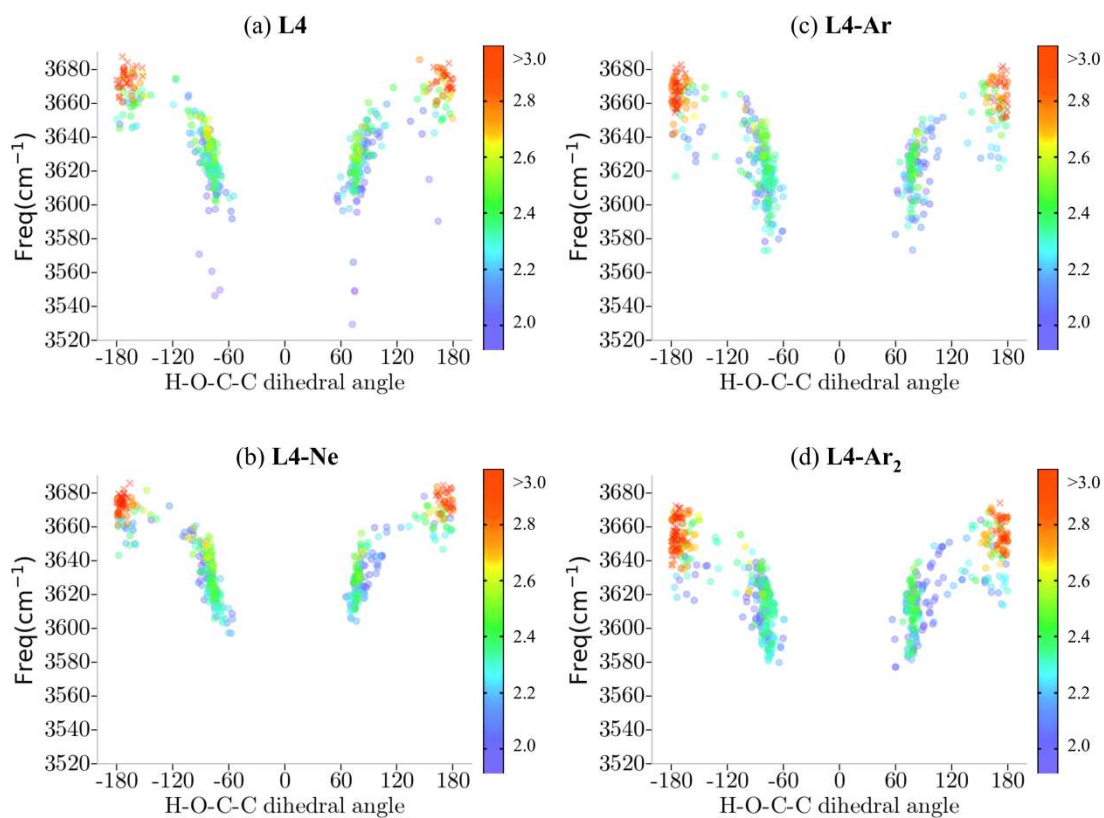


Figure S15. The H-O-C-C dihedral angles (abscissa) for the free OH sites versus free OH stretching frequencies (ordinate) in the stable **L** structures of (a) $\text{H}^+(\text{TFE})_4$, (b) $\text{H}^+(\text{TFE})_4\text{-Ne}$, (c) $\text{H}^+(\text{TFE})_4\text{-Ar}$, and (d) $\text{H}^+(\text{TFE})_4\text{-Ar}_2$ using M06-2X/6-311+G(d,p). The energies of the data points are within 5 kcal/mol to the most stable structure. The color code represents the distance between F and H atom of the free OH site as described in Figure S13. The red cross symbol represents the absence of the F atom to the free OH site using 3.5 Ångstrom as the cut-off distance.

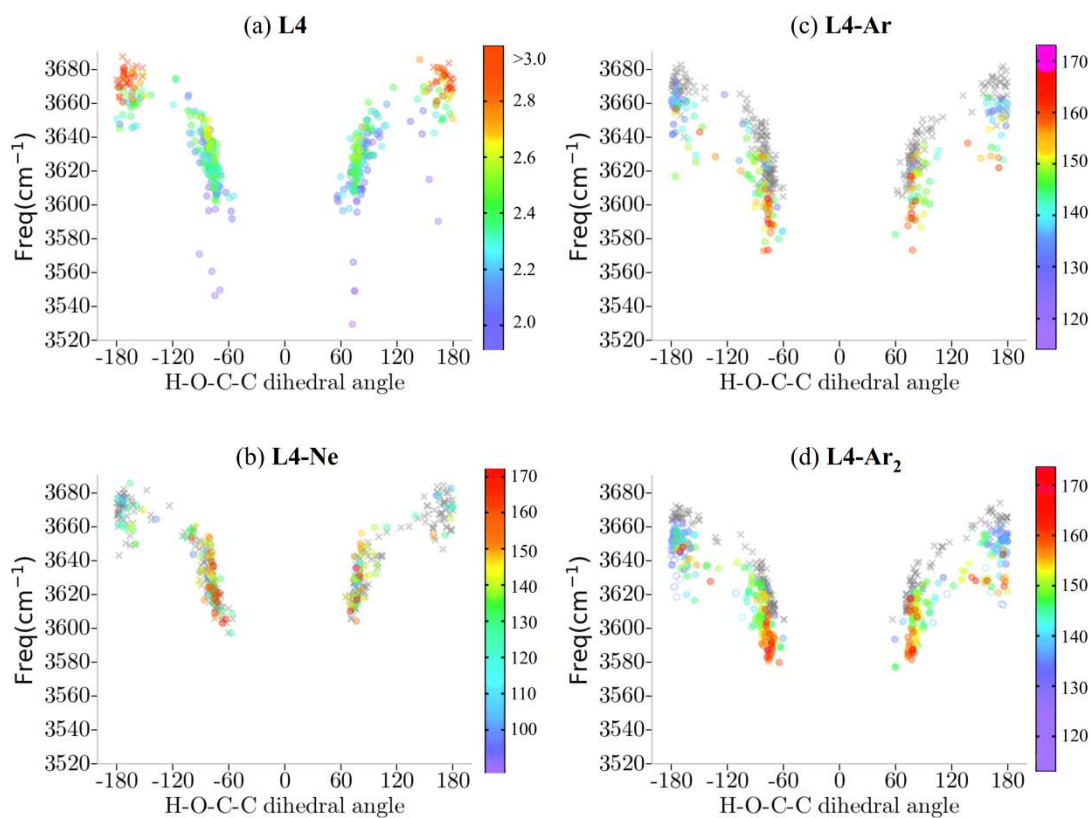


Figure S16. The H-O-C-C dihedral angles (abscissa) for the free OH sites versus free OH stretching frequencies (ordinate) in the stable **L** structures of (a) $\text{H}^+(\text{TFE})_4$, (same as Figure S15(a)) (b) $\text{H}^+(\text{TFE})_4\text{-Ne}$, (c) $\text{H}^+(\text{TFE})_4\text{-Ar}$, and (d) $\text{H}^+(\text{TFE})_4\text{-Ar}_2$ using M06-2X/6-311+G(d,p). The data points are the same as Fig. S15, but the definition of the color code in (b) – (d) is changed. The color code in (b) - (d) represents the X...H-O angles (X=Ne, Ar, or Ar₂) from smaller than 90 degrees for X=Ne and 130 degrees for X=Ar and Ar₂ (purple) to larger than 160 degrees (red). The gray cross symbol shows the absence of the tagged atom to the free OH site using 2.8 Ångstrom as the cut-off distance.

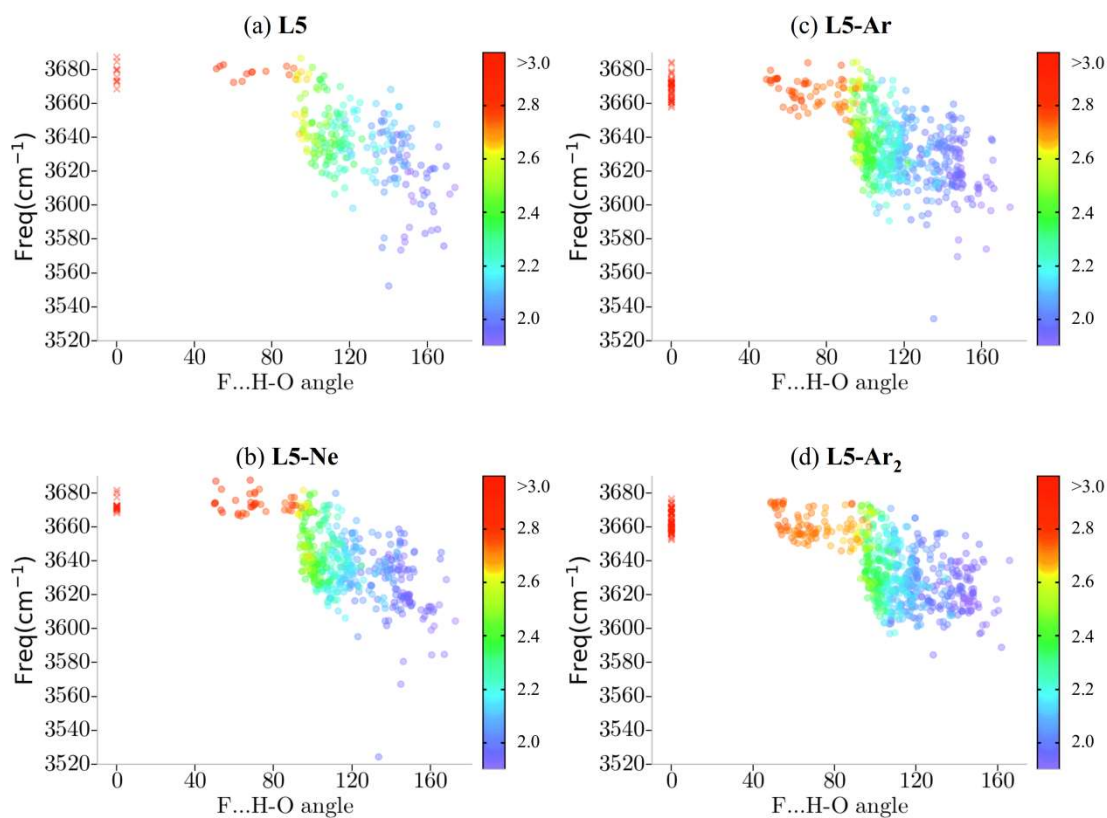


Figure S17. The F...H-O angles (abscissa) for the free OH sites versus free OH stretching frequencies (ordinate) in the stable L structures of (a) $\text{H}^+(\text{TFE})_5$, (b) $\text{H}^+(\text{TFE})_5\text{-Ne}$, (c) $\text{H}^+(\text{TFE})_5\text{-Ar}$, and (d) $\text{H}^+(\text{TFE})_5\text{-Ar}_2$ using M06-2X/6-311+G(d,p). The energies of the data points are within 5 kcal/mol to the most stable structure. The color code represents the distance between the F atom and the H atom of the free OH site from smaller than 2 Å (purple) to larger than 3 Å (red). The red cross symbol represents the absence of the F atom to the free OH site using 3.5 Å as the cut-off distance.

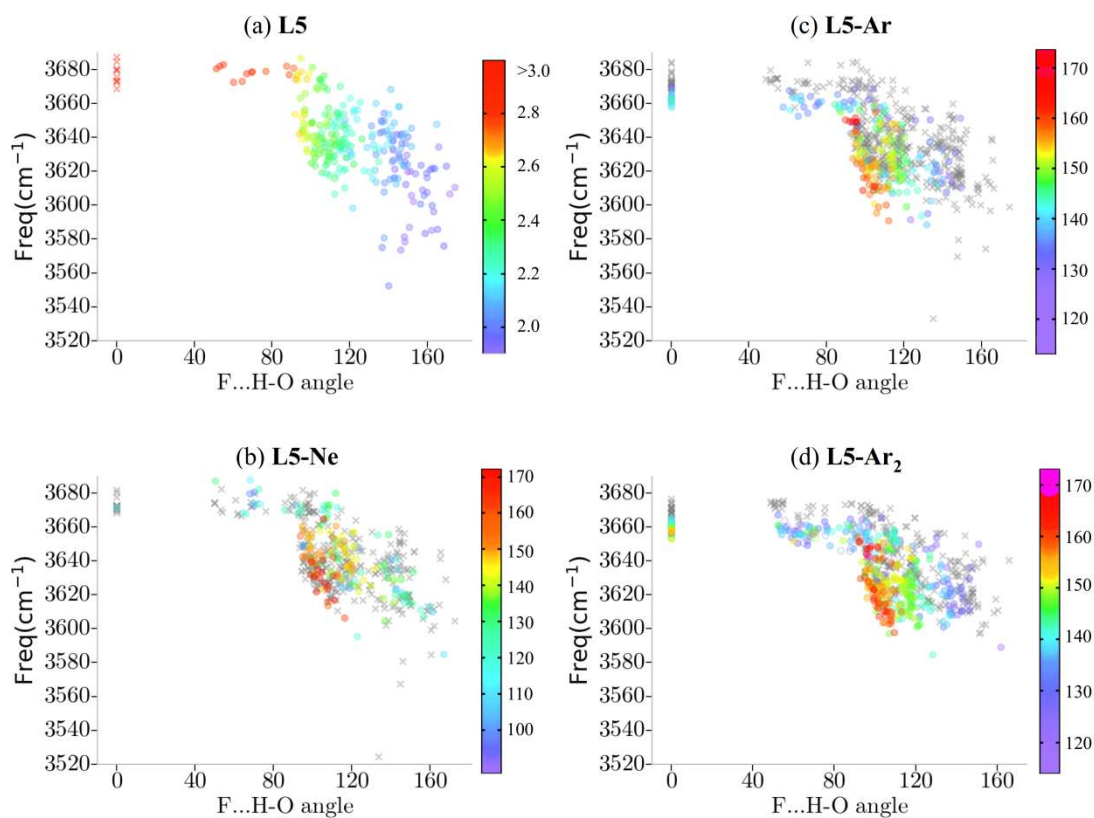


Figure S18. The F...H-O angles (abscissa) for the free OH sites versus free OH stretching frequencies (ordinate) in the stable L structures of (a) $\text{H}^+(\text{TFE})_5$ (same as Figure S17(a)), (b) $\text{H}^+(\text{TFE})_5\text{-Ne}$, (c) $\text{H}^+(\text{TFE})_5\text{-Ar}$ and (d) $\text{H}^+(\text{TFE})_5\text{-Ar}_2$ using M06-2X/6-311+G(d,p). The data points are the same as Fig. S17, but the definition of the color code in (b) – (d) is changed. The color code in (b) - (d) represents the X...H-O angles (X=Ne, Ar, or Ar₂) from smaller than 90 degrees for X=Ne and 130 degrees for X=Ar and Ar₂ (purple) to larger than 160 degrees (red). The gray cross symbol shows the absence of the tagged atom to the free OH site using 2.8 Ångstrom as the cut-off distance.

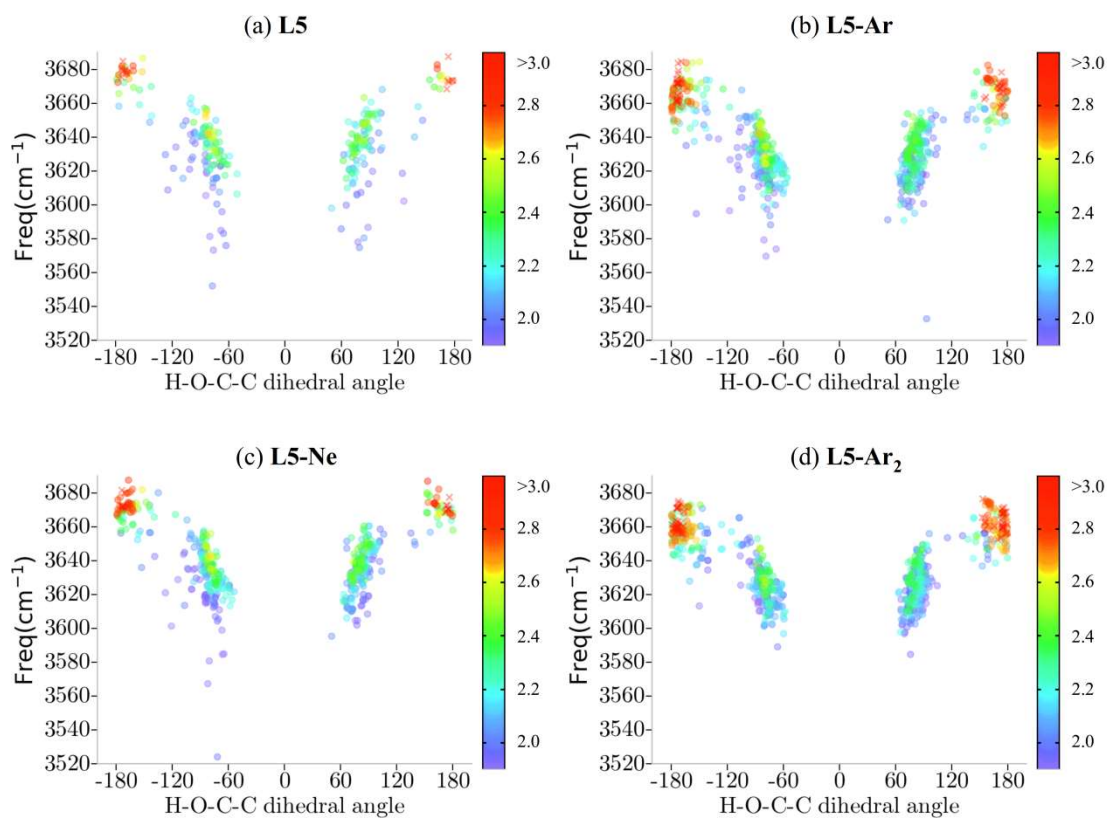


Figure S19. The H-O-C-C dihedral angles (abscissa) for the free OH sites versus free OH stretching frequencies (ordinate) in the stable **L** structures of (a) $\text{H}^+(\text{TFE})_5$, (b) $\text{H}^+(\text{TFE})_5\text{-Ne}$, (c) $\text{H}^+(\text{TFE})_5\text{-Ar}$, and (d) $\text{H}^+(\text{TFE})_5\text{-Ar}_2$ using M06-2X/6-311+G(d,p). The energies of the data points are within 5 kcal/mol to the most stable structure. The color code represents the distance between F and H atom of the free OH site as described in Figure S13. The red cross symbol represents the absence of the F atom to the free-OH site using 3.5 Å as the cut-off distance.

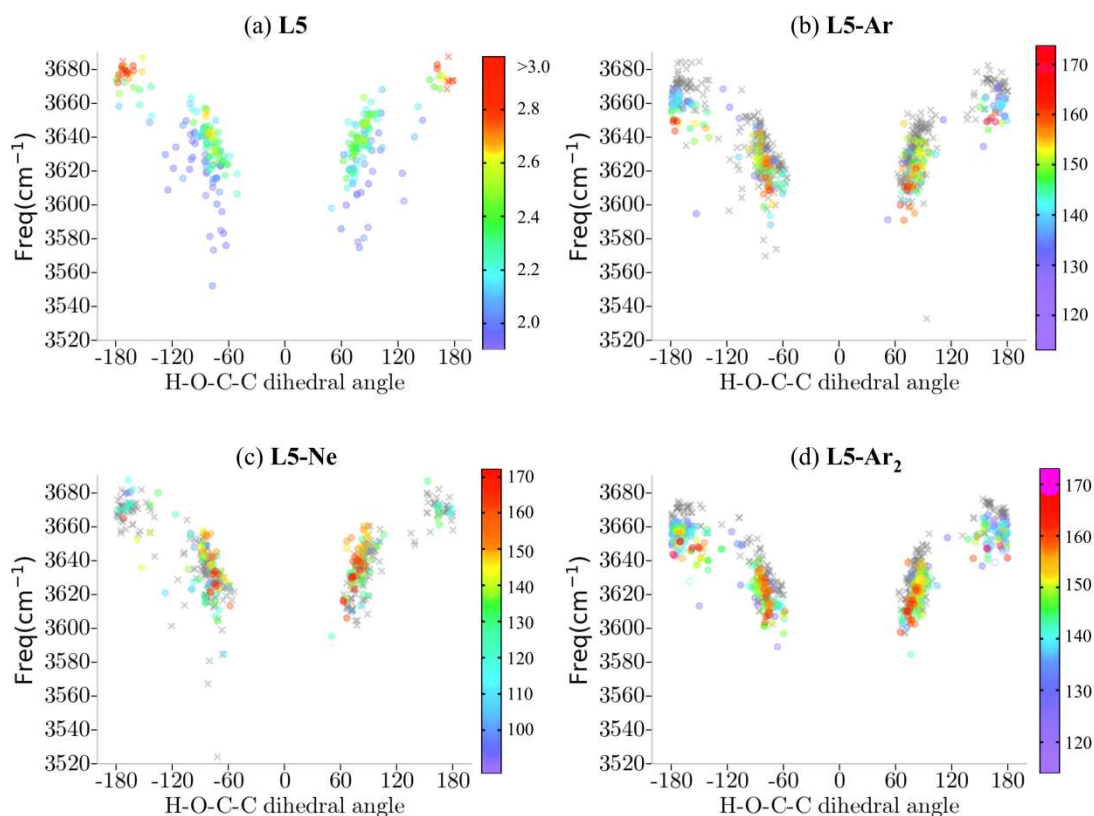


Figure S20. The H-O-C-C dihedral angles (abscissa) for the free OH sites versus free OH stretching frequencies (ordinate) in the stable L structures of (a) $\text{H}^+(\text{TFE})_5$, (same as Figure S19(a)) (b) $\text{H}^+(\text{TFE})_5\text{-Ne}$, (c) $\text{H}^+(\text{TFE})_5\text{-Ar}$, and (d) $\text{H}^+(\text{TFE})_5\text{-Ar}_2$ using M06-2X/6-311+G(d,p). The data points are the same as Fig. S19, but the definition of the color code in (b) – (d) is changed. The color code in (b) - (d) represents the X...H-O angles (X=Ne, Ar, or Ar₂) from smaller than 90 degrees for X=Ne and 130 degrees for X=Ar and Ar₂ (purple) to larger than 160 degrees (red). The gray cross symbol shows the absence of the tagged atom to the free OH site using 2.8 Å as the cut-off distance.

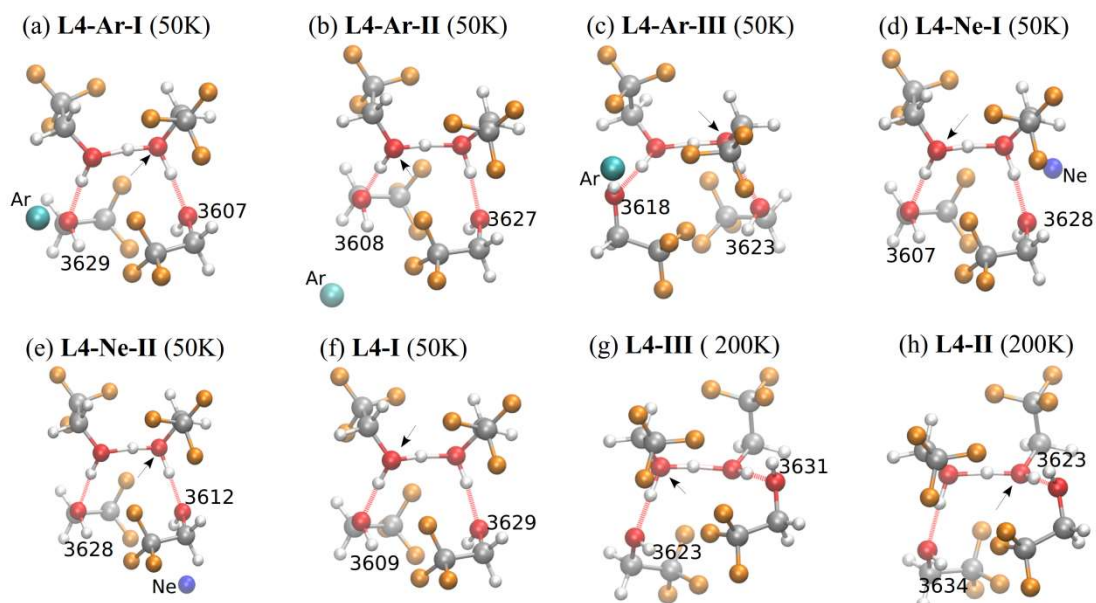


Figure S21. The structures of bare and tagged $\text{H}^+(\text{TFE})_4$ clusters with minimum free energy using B3LYP+D3/6-31+G(d). The selected temperatures correspond to those in Figure S9. The arrow indicates the protonated site. The numbers near the free OH sites indicate the free OH stretching frequencies in the unit of cm^{-1} , scaled by 0.973.

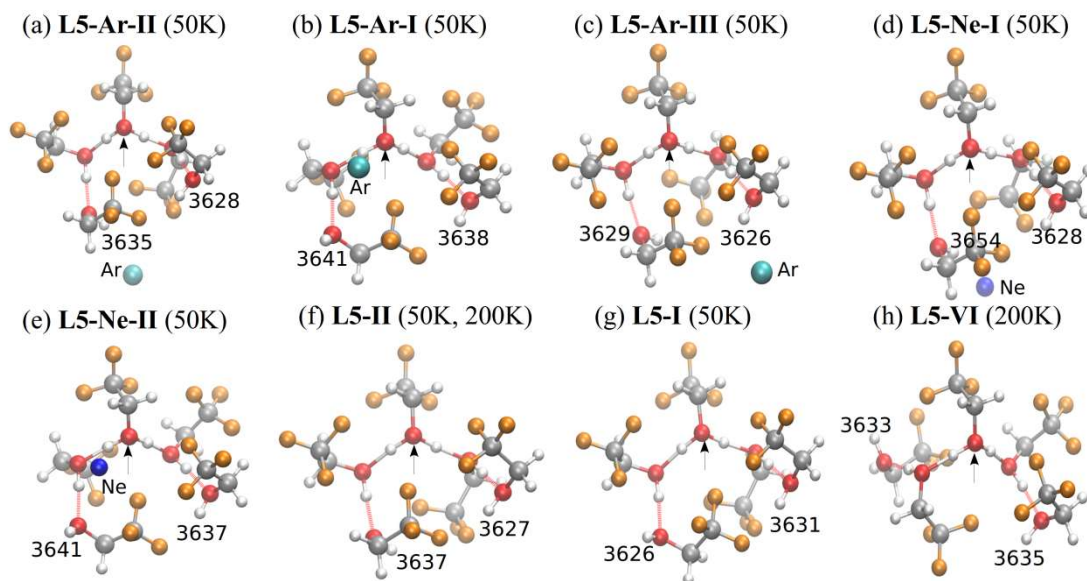


Figure S22. The structures of bare and tagged $\text{H}^+(\text{TFE})_5$ clusters with minimum free energy using B3LYP+D3/6-31+G(d). The selected temperatures correspond to those in Figure S10. The arrow indicates the protonated site. The numbers near the free OH sites indicate the free OH stretching frequencies in the unit of cm^{-1} , scaled by 0.973.

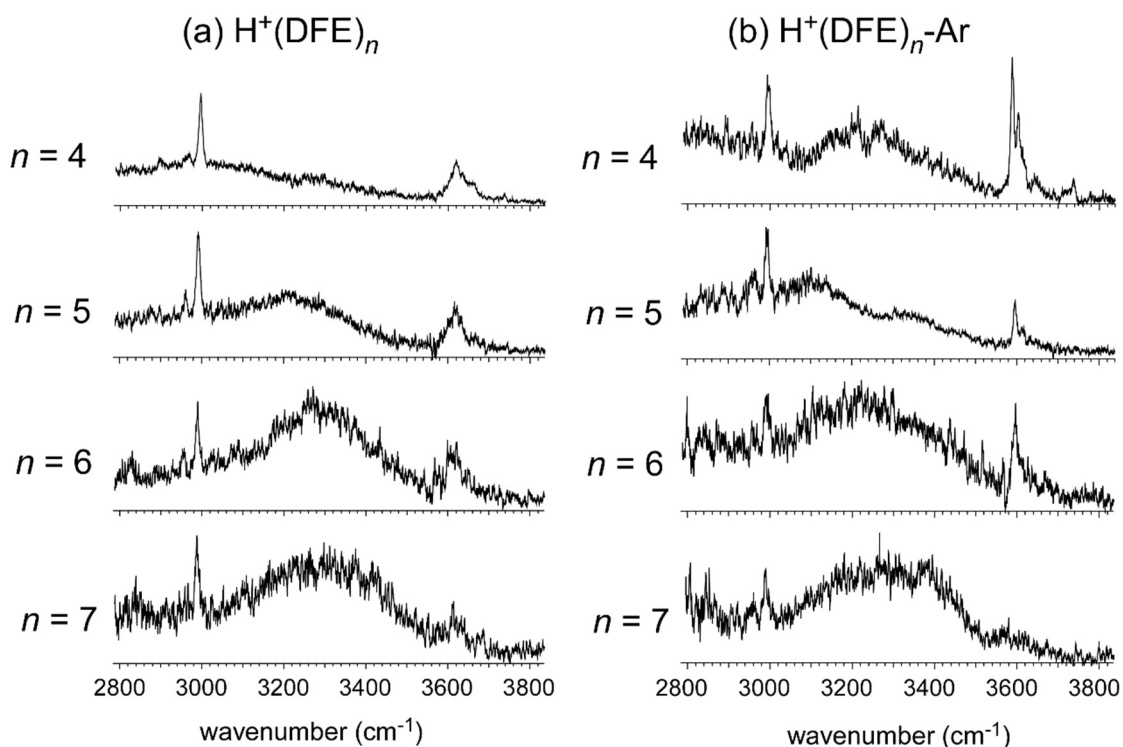


Figure S23. Infrared spectra of (a) $\text{H}^+(\text{DFE})_n$ and (b) $\text{H}^+(\text{DFE})_n\text{-Ar}$ in the size range of $n = 4 - 7$. The spectral feature does not show essential changes upon the Ar-tagging. The similarity of the spectra with those of $\text{H}^+(\text{TFE})_n$ and $\text{H}^+(\text{TFE})_n\text{-Ar}$ indicates that $\text{H}^+(\text{DFE})_n$ also have the **L** type structures in this size range, irrespective to cluster temperature.